

This discussion paper is/has been under review for the journal Hydrology and Earth System Sciences (HESS). Please refer to the corresponding final paper in HESS if available.

# Evidence of non-Darcy flow and non-Fickian transport in fractured media at laboratory scale

C. Cherubini<sup>1</sup>, C. I. Giasi<sup>2</sup>, and N. Pastore<sup>2</sup>

<sup>1</sup>HydriSE, Institut Polytechnique LaSalle Beauvais, 19 rue Pierre Waguet, 60026 Beauvais Cedex, France

<sup>2</sup>Sezione di Ingegneria Geotecnica e Geoambientale – DICATECh, Politecnico di Bari, Via Orabona 4, 70100 Bari, Italy

Received: 2 November 2012 – Accepted: 27 December 2012 – Published: 10 January 2013

Correspondence to: C. Cherubini (claudia.cherubini@gmail.com)

Published by Copernicus Publications on behalf of the European Geosciences Union.

**HESSD**

10, 221–254, 2013

**Evidence of  
non-Darcy flow and  
non-Fickian transport  
in fractured media**

C. Cherubini et al.

Title Page

Abstract

Introduction

Conclusions

References

Tables

Figures

⏪

⏩

◀

▶

Back

Close

Full Screen / Esc

Printer-friendly Version

Interactive Discussion

## Abstract

Accurate predictions of solute propagation in fractured rocks are of particular importance when assessing exposure pathways through which contaminants reach receptors during a risk assessment procedure, as well as when dealing with cleanup and monitoring strategies.

The difficulty in modeling fractured media leads to the application of simplified analytical solutions that fail to reproduce flow and transport patterns in such complex geological formations.

A way for understanding and quantifying the migration of contaminants in groundwater systems is that of analyzing tracer transport.

Experimental data obtained under controlled conditions such as in a laboratory allow to increase the understanding of the fundamental physics of fluid flow and solute transport in fractures.

In this study laboratory hydraulic and tracer tests have been carried out on an artificially created fractured rock sample. The tests regard the analysis of the hydraulic loss and the measurement of breakthrough curves for saline tracer pulse inside a rock sample of parallelepiped ( $0.60 \times 0.40 \times 0.8$  m) shape. The effect of the experimental apparatus on flow and transport tests has been estimated. In particular the convolution theory has been applied in order to remove the effect of acquisition apparatus on tracer experiment.

The experimental results have shown evidence of a non-Darcy relationship between flow rate and hydraulic loss that is best described by Forchheimer's law.

The observed experimental breakthrough curves of solute transport have been modeled by the classical one-dimensional analytical solution for advection–dispersion equation (ADE) and the single rate mobile–immobile model (MIM). The former model does not fit properly the first arrival and the tail while the latter provides a very decent fit.

# HESSD

10, 221–254, 2013

## Evidence of non-Darcy flow and non-Fickian transport in fractured media

C. Cherubini et al.

Title Page

Abstract

Introduction

Conclusions

References

Tables

Figures

⏪

⏩

◀

▶

Back

Close

Full Screen / Esc

Printer-friendly Version

Interactive Discussion

## 1 Introduction

Proper management of groundwater resources requires an understanding of the processes that cause water contamination and affect the remediation of polluted aquifers (Cherubini et al., 2010; Cherubini and Pastore, 2011).

5 One way to estimate the potential transport of contaminants is by using tracers, which are substances that can track the movement of water in an aquifer and are easily detectable. Testing involves injecting tracers and then monitoring the tracer concentrations as a function of location and/or time. The transport parameters are estimated by generating a tracer “breakthrough curve” (BTC) at the observation point (e.g. the  
10 pumping well) as a function of time.

Because of high costs associated with field transport experiments, laboratory tests are often conducted to study contaminant transport in representative rock samples.

Another advantage of laboratory experiments is the ability to constrain test interpretations by controlling flow geometry and by isolating the effects of certain transport mechanisms, which can make the overall process of parameter estimation easier and  
15 the test interpretations less ambiguous.

Qian et al. (2011) carried out well-controlled laboratory experiments to investigate flow and transport in a single fracture under non-Darcy flow conditions. Non-Fickian transport was found to dominate with early first arrival and long tails. A mobile–  
20 immobile (MIM) model proved to fit both peak and tails of the observed BTCs better than the classical ADE model.

On the basis of this experience, in order to describe the solute transport under different flow velocities and fracture apertures, Chen et al. (2011) carried out a series of well  
25 controlled flow and tracer test experiments on an artificial Channeled Single Fracture (CSF) – a single fracture with contact in certain areas – constructed in the laboratory. The flow condition showed a non-Darcy feature (best described by the nonlinear Forchheimer equation) and the BTCs showed a non-Fickian nature of transport such

## Evidence of non-Darcy flow and non-Fickian transport in fractured media

C. Cherubini et al.

Title Page

Abstract

Introduction

Conclusions

References

Tables

Figures



Back

Close

Full Screen / Esc

Printer-friendly Version

Interactive Discussion

as early arrival of the peak value, long tailing and multi-peak phenomena. The results of this study showed that the ADE is not adequate to describe the BTCs in a CSF.

Sudicky et al. (1985) examined the migration of a non-reactive tracer in layered media under controlled laboratory conditions by conducting multiple tracer tests with a column containing stratified porous media. The experimental results showed strongly dispersed and skewed shape of the breakthrough curves in contrast to the symmetric and weakly dispersed concentration patterns typically associated with homogeneous media. Simulations of the experiments demonstrated that these tailing effects are the result of a transient redistribution of the tracer across the strata by transverse molecular diffusion and that local longitudinal dispersion is only of secondary importance as a spreading process in such systems. These findings were consistent with recent theoretical descriptions of dispersion in stratified aquifers.

Starr et al. (1985) carried out reactive tracer tests on the same column and found breakthrough curves that were similar in form to those reported in the preceding study for a nonreactive solute, but were delayed in the time of appearance, had a lower peak concentration, and were more highly dispersed. A mathematical model accounting for longitudinal advection in the sand layer, transverse diffusion in the silt layers, and retardation in both the sand and silt layers gave a good representation of the experimental data, however significant discrepancies existed between the measured and simulated results, with the discrepancies becoming greater at lower velocities. The less satisfactory agreement obtained in the latter study suggested that there is some physical or chemical aspect of the retardation process that was not adequately represented in the model.

Callahan et al. (2000) carried out laboratory experiments by means of multiple experimental tracer methods to determine fracture/matrix interactions and dispersion in artificially created fractured rock core of volcanic tuff. They affirmed that matrix diffusion serves to increase the transport time of solutes in dual porosity media by spreading mass away from the advecting region of the fractures. However, they also affirmed that the results of these short-term tests were probably influenced to some degree by

# HESSD

10, 221–254, 2013

## Evidence of non-Darcy flow and non-Fickian transport in fractured media

C. Cherubini et al.

Title Page

Abstract

Introduction

Conclusions

References

Tables

Figures



Back

Close

Full Screen / Esc

Printer-friendly Version

Interactive Discussion



---

**Evidence of  
non-Darcy flow and  
non-Fickian transport  
in fractured media**C. Cherubini et al.

---

[Title Page](#)[Abstract](#)[Introduction](#)[Conclusions](#)[References](#)[Tables](#)[Figures](#)[⏪](#)[⏩](#)[◀](#)[▶](#)[Back](#)[Close](#)[Full Screen / Esc](#)[Printer-friendly Version](#)[Interactive Discussion](#)

smaller-scale processes that should be minimal in field experiments, such as diffusion within the stagnant water in the fractures (“free-water diffusion”), caused by fracture aperture variability, that were more important at small timescales. Because free water diffusion coefficients are larger than matrix diffusion coefficients, this led to an overestimation of the amount of diffusive mass transfer (Callahan et al., 2000).

Leven et al. (2005) carried out tracer tests at bench scale on artificially fractured laboratory blocks using port-port connections in such a way as to create matrix-dominated and fracture-dominated ports. Breakthrough curves detected at matrix-dominated port connections were characterized by mainly broad and flat curves in contrast to breakthrough curves recorded at the outlet of direct fracture connections, which showed earlier first arrivals with much sharper and steeper concentration increases.

The authors attributed short breakthrough times to a fast transport of the tracer through the fracture system with a less pronounced interaction with the matrix. The broad and flat breakthrough of tracer was attributed to transport mainly through the matrix with dominant diffusive transport mechanisms. The presence of tails in the BTC curves was attributed to matrix diffusion and to differential advection, i.e. the existence of pathways of varying length through the dimensionality of the flow field (McDermott, 1999).

Rodrigues et al. (2008) carried out several small-scale (laboratory) tracer tests to analyze the advection and dispersion of different solutes in fractured media.

The results obtained with sodium chloride revealed differences between direct and reverse tests, due to its density higher than the water. As a consequence, in case of significant openings near the injection hole the solution might sink there initially and it was released later by diffusion. In case of no pits near the injection point then the solution could get mixed with the flowing water more easily and so it traveled faster through the system.

Thus, as the transport was found to depend on the morphology of the areas around the injection holes, the parameters calculated in the tests with sodium chloride did not correspond to the parameters of the flowing water.

On the other hand, the tests with fluorescein or sulphorhodamine allowed to obtain parameters characterizing the flow pattern without being affected by exogenous factors because they behaved as inert tracers showing advection-dominated transport with high Péclet numbers.

The present study uses well-controlled laboratory experiments to investigate flow and transport in an artificially fractured laboratory block. Flow in the experiments is nonlinear and is well described by the Forchheimer equation (Cherubini et al., 2012). Non-Fickian transport is found to dominate with early first arrival and long tails. The breakthrough curves (BTCs) of the solute transport are modeled by the conventional advection–dispersion equation (ADE), and the single rate mobile–immobile (MIM) model. The former poorly describes the behavior of the breakthrough curves while the latter is able to fit the peak value and the tail.

## 2 Theoretical background

### 2.1 Flow models

Generally the model used to describe fluid flow in fractured media is the local Cubic law which adapts Darcy law under the assumption of ideal fractures with flat, smooth and parallel walls with infinite lengths, together with laminar flow, incompressible fluid and confined configuration. Different studies in literature show that in real rock fractures a nonlinear flow behavior is easy to occur. A flow model commonly used to represent non-Darcy flow behavior is the Forchheimer law which includes a quadratic term of velocity to represent the inertial effect:

$$-\frac{dh}{dx} = av + bv^2 \quad (1)$$

where  $h$  (L) is the hydraulic head,  $x$  (L) is the spatial coordinate along the direction of the flow,  $v$  ( $LT^{-1}$ ) is the flow velocity,  $a$  ( $TL^{-1}$ ) and  $b$  ( $T^2L^{-2}$ ) are the linear and inertial coefficients, respectively.

## Evidence of non-Darcy flow and non-Fickian transport in fractured media

C. Cherubini et al.

Title Page

Abstract

Introduction

Conclusions

References

Tables

Figures

⏪

⏩

◀

▶

Back

Close

Full Screen / Esc

Printer-friendly Version

Interactive Discussion



A general Darcian-like relationship can be used to describe nonlinear flow regimes:

$$v = -K_{\text{eff}} \left( \frac{dh}{dx} \right) \frac{dh}{dx} \quad (2)$$

$K_{\text{eff}}$  ( $\text{LT}^{-1}$ ) represents the effective hydraulic conductivity function of hydraulic gradient. According to Forchheimer law, the effective hydraulic conductivity can be written as:

$$K_{\text{eff}} = \frac{2}{a + \sqrt{a^2 + 4b \left| \frac{dh}{dx} \right|}} \quad (3)$$

## 2.2 Solute transport models

One of the most widely used solute transport models in field applications reported in literature is the Advection Dispersion Equation (ADE). The ADE model is based on Fick's law which assumes that the dispersive mass flux is proportional to the first-order spatial derivative of concentration (Bear, 1972). The mathematical formulation of the ADE model for non-reactive solute transport can be expressed as follows:

$$\frac{\partial c}{\partial t} = D \frac{\partial^2 c}{\partial x^2} - v \frac{\partial c}{\partial x} \quad (4)$$

where  $t$  (T) is the time,  $x$  (L) is the spatial coordinate along the direction of the flow,  $c$  ( $\text{ML}^{-3}$ ) is the solute concentration,  $v$  ( $\text{LT}^{-1}$ ) is the average flow velocity and  $D$  ( $\text{L}^2\text{T}^{-1}$ ) is the dispersion coefficient. In complex fractured media the latter depends mainly on two processes: Taylor–Aris dispersion ( $D_T$ ) due to the combined action of convection and radial molecular diffusion (Dullien, 1992) and geometrical dispersion ( $D_G$ ) due to the roughness and/or aperture-variation of fractures (Boschan et al., 2008). For a fracture characterized by two flat parallel walls geometrical dispersion should be equal to zero and dispersion processes are represented only by Taylor–Aris dispersion by the

## Evidence of non-Darcy flow and non-Fickian transport in fractured media

C. Cherubini et al.

Title Page

Abstract

Introduction

Conclusions

References

Tables

Figures

⏪

⏩

◀

▶

Back

Close

Full Screen / Esc

Printer-friendly Version

Interactive Discussion



following expression:

$$D_T = \frac{2}{105} \frac{v^2 w^2}{D_m} \quad (5)$$

where  $w$  (L) is aperture of fracture,  $D_m$  ( $L^2 T^{-1}$ ) is the molecular diffusion.

Geometrical dispersion is nonzero only for fracture with rough walls and/or with variable aperture and reflects the influence of spatial variation of flow velocity in the plane of fractures. The geometrical dispersion resulting from heterogeneity along the fracture plane varies linearly with the mean velocity:

$$D_G = \alpha_L v \quad (6)$$

where  $\alpha_L$  (L) is the geometrical dispersivity coefficient.

The Péclet number is defined as:

$$Pe = \frac{v w}{D_m} \quad (7)$$

can be used to distinguish different regimes in variable aperture fractures: molecular diffusion, geometric dispersion and Taylor–Aris dispersion. The geometric dispersion regime corresponds to the range of  $Pe$  where velocity variations in the plane of fractures dominate the mixing process. This means that for low values of  $\alpha_L$  the dispersion passes directly from the molecular diffusion regime to the Taylor–Aris dispersion regime whereas for high values of  $\alpha_L$  there exists a large range of  $Pe$  in which geometrical dispersion dominates.

Péclet number is also defined as:

$$Pe = \frac{v L}{D} \quad (8)$$

where  $L$  (L) is the characteristic length of the domain. It represents the relative effect of advective compared to dispersive solute transport. At high Péclet numbers  $Pe \gg 1$

## Evidence of non-Darcy flow and non-Fickian transport in fractured media

C. Cherubini et al.

Title Page

Abstract

Introduction

Conclusions

References

Tables

Figures

⏪

⏩

◀

▶

Back

Close

Full Screen / Esc

Printer-friendly Version

Interactive Discussion



advection dominates solute transport processes; while at low Péclet numbers  $Pe < 1$  dispersion/diffusion dominates.

In a typical tracer injection experiment a mass  $M_0$  (M) of the tracer is injected instantaneously at time zero at the origin of the domain ( $x = 0$ ). The initial condition is given by:

$$c(x, t = 0) = \frac{M}{\omega} \delta(x) \quad (9)$$

where  $\omega$  ( $L^2$ ) is the cross sectional area,  $\delta(x)$  ( $L^{-1}$ ) is the Dirac-delta, which is equal to 1 when  $x$  is equal to zero and is 0 otherwise.

In addition, it is assumed that a first-type boundary condition exists at the outflow boundary:

$$c(\pm\infty, t) = 0 \quad (10)$$

The solution of Eq. (4) for the specified initial and boundary conditions is given by (Crank, 1956):

$$c_0(x, t) = \frac{M}{\omega \sqrt{\pi D_t}} e^{-\frac{(x-vt)^2}{4D_t}} \quad (11)$$

The mobile-immobile model (MIM) assumes that the net mass transfer from the main flow field to the stagnation zones is proportional to the difference of concentration between the mobile and immobile domain. The mathematical formulation of the MIM for non-reactive solute transport is usually given as follows:

$$\begin{aligned} \frac{\partial c_m}{\partial t} &= D \frac{\partial^2 c_m}{\partial x^2} - v \frac{\partial c_m}{\partial x} - \alpha (c_m - c_{im}) \\ \beta \frac{\partial c_{im}}{\partial t} &= \alpha (c_m - c_{im}) \end{aligned} \quad (12)$$

## Evidence of non-Darcy flow and non-Fickian transport in fractured media

C. Cherubini et al.

Title Page

Abstract

Introduction

Conclusions

References

Tables

Figures

◀

▶

◀

▶

Back

Close

Full Screen / Esc

Printer-friendly Version

Interactive Discussion



where  $c_m$  and  $c_{im}$  are the cross-sectional averaged solute concentrations respectively in the mobile and immobile domain,  $\alpha$  ( $T^{-1}$ ) is the mass exchange coefficient,  $\beta$  (–) is the mobile water fraction.

The Damköhler (Da) number can be used to evaluate the behavior of MIM model, but it has been showed that there are limitations to a tracer test's ability to estimate the exchange parameters  $\alpha$  and  $\beta$ .

This dimensionless number can be expressed as (Wagner and Harvey, 2001):

$$Da = \frac{\alpha(1 + \beta)L}{v} \quad (13)$$

At high values of Da the solute concentrations in mobile and immobile domain are in equilibrium and MIM tends to ADE model. In this case the effect of the exchange is difficult to identify. At very low value of Da the mass transfer is absent or very slow and a dual domain performs as a single domain. Only a small amount of tracer interacts with the immobile zones thus the exchange effect is small and difficult to identify. In between these values of Da the mass transfer is controlled by a first order kinetic process depending on the concentration gradient between the mobile and the immobile domain (Eq. 10). Bahr and Rubin (1987) demonstrated the use of this dimensionless number for identifying those cases where non-equilibrium transport cannot be distinguished from equilibrium transport.

In analogous manner for the ADE model the solution of system Eq. (10) describing one-dimensional non-reactive solute transport in an infinite domain for instantaneous pulse of solute injected at time zero at the origin is given by (Goltz and Roberts, 1986):

$$c_1(x, t) = e^{-\alpha t} c_0(x, t) + \alpha \int_0^t H(t, \tau) c_0(x, \tau) d\tau \quad (14)$$

with:

**Evidence of non-Darcy flow and non-Fickian transport in fractured media**

C. Cherubini et al.

Title Page

Abstract

Introduction

Conclusions

References

Tables

Figures

⏪

⏩

◀

▶

Back

Close

Full Screen / Esc

Printer-friendly Version

Interactive Discussion



$$H(t, \tau) = e^{-\frac{\alpha}{\beta}(t-\tau) - \alpha\tau} \frac{\tau I_1 \left( \frac{2\alpha}{\beta} \sqrt{\beta(t-\tau)\tau} \right)}{\sqrt{\beta(t-\tau)\tau}} \quad (15)$$

where  $I_1$  represents the modified Bessel function of order 1.

In order to simplify the calculation of the analytical solutions a unit length for the one-dimensional domain has been assumed. It is therefore necessary to normalize the parameters  $\nu$  and  $D$  so they both have units of ( $T^{-1}$ ). To obtain the normalized values of  $\nu$  and  $D$ , it is simply necessary to multiply them by  $L$  and  $L^2$  respectively.

### 2.3 Convolution solutions for variable boundary conditions

The transport solution presented in the previous sections allows the determination and the prediction of breakthrough curves (BTCs) at a specified distance from the inlet boundary. This solution assumes instantaneous pulse injection input condition. In many experimental systems the input boundary condition could be different or the transport occurs through regions with distinctly different properties (Berkowitz et al., 2001). Generally in field scale both the injection time and the residence time of the solute within the probe are negligible compared to the residence time of solute in the aquifer. Instead in laboratory scale these assumptions could not be valid because the residence times of the solute in the medium and in the probe are of the same order of magnitude. Convolution techniques can be used to overcome these problems.

Given the BTC curves for the medium  $C(t)$  and for the probe  $S(t)$  corresponding to the analytical solutions for a pulse input, the convolution of  $C(t)$  and  $S(t)$  is formally defined as:

$$W(t) = C(t) \cdot S(t) = \int_0^t C(t-\tau)S(\tau)d\tau \quad (16)$$

where  $W(t)$  is the resulting breakthrough curve recorded by the probe.

## Evidence of non-Darcy flow and non-Fickian transport in fractured media

C. Cherubini et al.

Title Page

Abstract

Introduction

Conclusions

References

Tables

Figures

⏪

⏩

◀

▶

Back

Close

Full Screen / Esc

Printer-friendly Version

Interactive Discussion



### 3 Materials and methods

#### 3.1 Experimental setup

The experiments have been performed on a limestone block with parallelepiped shape ( $0.6 \times 0.4 \times 0.08 \text{ m}^3$ ) recovered from the “Calcarea di Altamura” formation which is located in Apulia region in southeastern Italy (Cherubini et al., 2012).

The fracture network has been made artificially through 5 kg mallet blows (Fig. 1a). The fissured system and the fracture aperture on the block surfaces have been recorded with a high resolution digital camera. Subsequently the images have been scaled and rectified using “Perspective Rectifier” (<http://www.rectifiersoft.com>) and calibrated on the basis of manual measurements carried out by means of a caliber. Profiles of discontinuities and aperture measurements have been extracted from the recorded images using “edge” function with “canny” filter from the built-in “Scilab Image Processing Toolbox” (<http://www.scilab.org>). For each discontinuity the median profile and the aperture distribution have been determined.

The surface of the block sample has been sealed with transparent epoxy resin (Leven et al., 2004) (Fig. 1b). A hole of 1 cm diameter has been opened for each discontinuity in correspondence of the boundary of the block by means of a percussion drill (Fig. 1c). Inside each hole an hexagonal bushing of  $1/4'' \text{ M}-3/8'' \text{ F}$  has been placed and welded to the block by means of rapid-hardening epoxy resin (Fig. 1d).

In the present paper the study of flow and transport dynamics regards only a single path. Figure 2a shows the mechanical aperture distribution obtained from 13688 measurements and Fig. 2b shows the reconstructed three-dimensional geometry of the selected path. The average cross-sectional area of the path is equal to  $\bar{\omega} = 0.9932 \text{ mm}^2$  whereas the average path length is equal to  $\bar{L} = 0.7531 \text{ m}$ .

The sealed block sample is connected with a hydraulic circuit (Fig. 3). Water inside the block flows according to the hydraulic head difference between the upstream tank connected to the inlet port and the downstream tank connected to the outlet port. The upstream and downstream tanks have the same dimensions and are of cylindrical

## Evidence of non-Darcy flow and non-Fickian transport in fractured media

C. Cherubini et al.

Title Page

Abstract

Introduction

Conclusions

References

Tables

Figures

⏪

⏩

◀

▶

Back

Close

Full Screen / Esc

Printer-friendly Version

Interactive Discussion



shape with a circular cross section. The instantaneous flow rate that flows across the block is measured by an ultrasonic velocimeter (DOP3000 SIGNAL PROCESSING). In correspondence of the inlet port a syringe for instantaneous injection of a conservative tracer (sodium chloride, NaCl) is placed while in correspondence of the outlet port a flow cell is placed in which a probe can be positioned. The probe is a multi-parametric instrument (IDRONAUT OCEAN SEVEN 304 CTD LOGGER) with frequency of sampling 8 Hz for instantaneous measurement of pressure (dbar), temperature ( $^{\circ}\text{C}$ ) and electric conductivity ( $\mu\text{Scm}^{-1}$ ) respectively with resolution 0.0015%, 0.0006 $^{\circ}\text{C}$  and 0.1  $\mu\text{Scm}^{-1}$ .

### 3.2 Flow tests

The analysis of flow dynamics through the selected path regards the observation of water flow from the upstream tank to the flow cell with a circular cross-section of 0.1963 m<sup>2</sup> and  $1.28 \times 10^{-4}$  m<sup>2</sup>, respectively.

Initially at time  $t_0$ , the valves “a” and “b” are closed and the hydrostatic head in the flow cell is equal to  $h_0$ . The experiment begins with the opening of the valve “a” which is reclosed when the hydraulic head in the flow cell is equal to  $h_1$ . Finally the hydraulic head in the flow cell is reported to  $h_0$  through the opening of the valve “b”. The experiment procedure is repeated changing the hydraulic head of the upstream tank  $h_c$ . The time  $\Delta t = (t_1 - t_0)$  required to fill the flow cell from  $h_0$  to  $h_1$  has been registered.

Given that the capacity of the upstream tank is much higher than that of the flow cell it is reasonable to assume that during the experiments the level of the upstream tank remains constant. Under this hypothesis the flow inside the system is governed by the equation:

$$S_1 \frac{dh}{dt} = \Gamma(\Delta h)(h_c - h) \quad (17)$$

## Evidence of non-Darcy flow and non-Fickian transport in fractured media

C. Cherubini et al.

Title Page

Abstract

Introduction

Conclusions

References

Tables

Figures

⏪

⏩

◀

▶

Back

Close

Full Screen / Esc

Printer-friendly Version

Interactive Discussion



where  $S_1$  ( $L^2$ ) and  $h$  ( $L$ ) are respectively the section area and the hydraulic head of the flow cell;  $h_c$  ( $L$ ) is the hydraulic head of upstream tank,  $\Gamma(\Delta h)$  represent the hydraulic conductance term representative of both hydraulic circuit and the selected path.

Hydraulic loss within the single hydraulic circuit can be expressed according to Chezy law as:

$$Q = C \sqrt{|\Delta h|} \Rightarrow \Delta h = \frac{1}{C^2} Q^2 \Rightarrow \Delta h = R_c Q^2 \quad (18)$$

where  $R_c$  ( $T^2 L^{-5}$ ) is a characteristic coefficient related to the roughness, section and length of the tubes of the hydraulic circuit.

Whereas, only for the sealed block,  $\Delta h$ - $Q$  relationship can be expressed by means of a discrete form of Forchheimer law:

$$\Delta h = A \cdot Q + B \cdot Q^2 \quad (19)$$

where  $A$  ( $TL^{-2}$ ) and  $B$  ( $T^2 L^{-5}$ ) are the linear and nonlinear hydraulic loss coefficients respectively and are related to the roughness, aperture, lengths and shape of the selected path in the fractured medium.

Combining Eqs. (16) and (17) the hydraulic conductance term of the whole hydraulic system assumes the following expression:

$$\Gamma(\Delta h) = \frac{2}{A + \sqrt{A^2 + 4(B + R_c)|\Delta h|}} \quad (20)$$

The average flow rate can be estimated by means of the volumetric method:

$$\bar{Q} = \frac{S_1}{t_1 - t_0} (h_1 - h_0) \quad (21)$$

Whereas the average head difference is given by:

$$\overline{\Delta h} = h_c - \frac{h_0 + h_1}{2} \quad (22)$$

**Evidence of non-Darcy flow and non-Fickian transport in fractured media**

C. Cherubini et al.

Title Page

Abstract

Introduction

Conclusions

References

Tables

Figures

⏪

⏩

◀

▶

Back

Close

Full Screen / Esc

Printer-friendly Version

Interactive Discussion



In correspondence of the average flow rate and head difference is it possible to evaluate the average hydraulic conductance as:

$$\bar{\Gamma}(\Delta h) = \frac{S_1}{t_1 - t_0} \ln \left( \frac{h_0 - h_c}{h_1 - h_c} \right) \quad (23)$$

The inverse of  $\bar{\Gamma}(\Delta h)$  represents the average resistance to flow.

Substituting Eq. (18) into Eq. (15) and integrating the latter from  $t = t_0$  to  $t = t_1$  with the initial condition  $h = h_0$  the following expression is obtained for Forchheimer's law:

$$S_1 \left( -\sqrt{A^2 + 4(B + R_c)(h_c - h)} - A \ln \left( \sqrt{A^2 + 4(B + R_c)(h_c - h)} - A \right) \right) \Big|_{h_0}^{h_1} = t_1 - t_0 \quad (24)$$

By fitting the experimental relation between  $\Delta t = t_1 - t_0$  and  $h_c$  it is possible to obtain an estimation of the coefficients  $A$  and  $B$ .

### 3.3 Tracer tests

The study of solute transport dynamics through the selected path has been carried out by means of a tracer test using sodium chloride. Initially a hydraulic head difference between the upstream tank and downstream tank is imposed. At  $t = 0$  the valve "a" is closed and the hydrostatic head inside the block is equal to the upstream tank. At  $t = 10$  s the valve "a" is opened while at time  $t = 60$  s a mass of solute equal to  $5 \times 10^{-4}$  kg is injected into the inlet port through a syringe. The source release time (1 s) is very small therefore the instantaneous source assumption can be considered valid.

In correspondence of the flow cell in which the multi-parametric probe is located it is possible to measure the breakthrough curve of the tracer and the hydraulic head; in the meanwhile the flow rate entering the system is measured by means of ultrasonic velocimeter. For different flow rates a BTC curve can be recorded in correspondence of outlet port.

## Evidence of non-Darcy flow and non-Fickian transport in fractured media

C. Cherubini et al.

Title Page

Abstract

Introduction

Conclusions

References

Tables

Figures

⏪

⏩

◀

▶

Back

Close

Full Screen / Esc

Printer-friendly Version

Interactive Discussion





is linear and the estimated volume of flow cell Vol is  $1.237 \times 10^{-4} \text{ m}^3$ , close to the real volume of flow cell equal to  $1.417 \times 10^{-4} \text{ m}^3$ .

## 4.2 Flow characteristics

Several tests have been conducted for the selected path. The control head  $h_c$  varies in the range of 0.17–1.37 m and the average flow rates observed are the range of  $1.85 \times 10^{-6}$ – $1.11 \times 10^{-5} \text{ m}^3 \text{ s}^{-1}$ . Figure 6 shows the fitting method described in previous section to estimate the linear and nonlinear terms equal to  $A = 4.11 \times 10^4$  and  $B = 6.61 \times 10^9$ , respectively.

## 4.3 Solute transport

Several tests have been conducted for the selected path in order to observe solute transport behavior varying the flow rate in the range  $1.20 \times 10^{-6}$ – $8.34 \times 10^{-6} \text{ m}^3 \text{ s}^{-1}$ . Each obtained experimental BTC curve has been fitted with ADE and MIM model, respectively.

Figure 7 shows the Root Mean Square Error (RMSE) of the fitting procedure for ADE and MIM models varying the flow rate. The MIM model has lower RMSE values than ADE. In particular way the latter shows maximum RMSE values for  $4 \times 10^{-6} \text{ m}^3 \text{ s}^{-1} < Q < 6 \times 10^{-6} \text{ m}^3 \text{ s}^{-1}$ .

Figure 8 shows the measured BTCs fitted by ADE and MIM models simultaneously for given average flow rates of  $5.98 \times 10^{-6}$ ,  $2.54 \times 10^{-6}$ ,  $1.84 \times 10^{-6}$  and  $1.32 \times 10^{-6} \text{ m}^3 \text{ s}^{-1}$ .

The MIM model proves to fit adequately the observed BTCs. However, especially for low values of flow rate the MIM model does not fit precisely the experimental BTCs, in fact a “late peak” is observed. As the one-dimensional analytical model is not able to fit properly, maybe an accurate method (see Bodin et al., 2007) could be more adequate. Nevertheless, the causes of this phenomenon may be subject of further studies.

## Evidence of non-Darcy flow and non-Fickian transport in fractured media

C. Cherubini et al.

Title Page

Abstract

Introduction

Conclusions

References

Tables

Figures

⏪

⏩

◀

▶

Back

Close

Full Screen / Esc

Printer-friendly Version

Interactive Discussion

In order to individuate the transition between viscous and inertial dominating regime in Fig. 9 are plotted the ratios of linear and non linear losses to total head loss. In correspondence of  $Q = 6.4 \times 10^{-6} \text{ m}^3 \text{ s}^{-1}$  inertial effects prevail on viscous ones.

On the same diagram the experimental relationships of flow rate and normalized velocity for ADE and MIM models have been superimposed.

In the transition between viscous and inertial regime a change in the slope can be evidenced, which means a different behavior. In physical terms this means that the diagram of velocity profile is flattened because of inertial forces prevailing on viscous ones. While the presence of a transitional flow regime does not exert influence on the behavior of dispersion. In fact in Fig. 10 it is shown the relationship between velocity and dispersion for both ADE and MIM models. In both cases a linear relationship is evidenced, the ADE overestimating the dispersion respect to MIM. This finding is coherent with the results of Detwiler et al. (2000) who found three different dispersive regimes on the basis of Péclet number described by Eq. (7). In our study the linear relationship between  $v$  and  $D$  depicts a geometrical dispersion dominant regime.

In Fig. 11 the first order mass exchange term  $\alpha$  of the MIM model is plotted as function of the normalized velocity ( $v/\bar{L}$ ). For low normalized velocity values  $\alpha$  is constant, while in correspondence of the  $v/\bar{L} = 1.5 \times 10^{-2} \text{ s}^{-1}$  it increases linearly. The mobile water fraction  $\beta$  coefficient shows a constant mean value of 0.56 for all velocity ranges.

In Fig. 12 the Damköhler number is plotted as function of Péclet number (Eq. 8). For the analyzed range of flow rates, the Péclet number varies in the range 5–15 (advective dominant regime) and the Damköhler number in the range 0.4–1, meaning that mass exchange between the two domains is not negligible.

For the range of analyzed flow rates, the regression of the curve has a constant slope, that means a constant ratio of Damköhler and Péclet numbers, that is to say a constant value of the product  $\alpha D v^{-2}$ .

## Evidence of non-Darcy flow and non-Fickian transport in fractured media

C. Cherubini et al.

Title Page

Abstract

Introduction

Conclusions

References

Tables

Figures

⏪

⏩

◀

▶

Back

Close

Full Screen / Esc

Printer-friendly Version

Interactive Discussion



## 5 Conclusions

Solute transport in fractured media becomes a big issue in hydrogeologic engineering when dealing with groundwater reservoir finding, nuclear waste disposal, risk assessment and cleanup and monitoring strategies (Cherubini and Pastore, 2010). A way for understanding the migration of contaminants in such complex systems is that of analyzing tracer transport. In this paper controlled laboratory experiments on flow and transport have been carried out at bench scale in an artificially fractured limestone block.

For a selected path both hydraulic and pulse tracer tests have been conducted. Hydraulic tests have proved the existence of a nonlinear flow behavior best described by the Forchheimer's law.

The observed experimental breakthrough curves obtained from pulse injection tests varying the flow rate have been modeled by two models, the conventional one-dimensional analytical ADE and the MIM model. The former poorly describes the behavior of BTC while the latter is able to fit the peak value and the tail. For all tracer tests performed the RMSE between observed and modeled BTCs of the MIM model is always smaller than that of the ADE model.

All experimental BTCs exhibit a non-Gaussian distribution with a long tail and demonstrate the non-Fickian nature of transport. The ADE approach implemented on a flow model calibrated on the hydraulic tests has done a poor job in explaining the solute transport as it fails to fit the peak and the tail of BTCs. In order to fit experimental BTCs, the ADE model tends to underestimate the velocity and overestimate the dispersion coefficient respect to the MIM model.

The relationships between the flow rate and the normalized velocity estimated for ADE and MIM model show a change in the slope in correspondence of the transition from dominant viscous regime to inertial regime. This phenomenon can be ascribed to the flattening of the diagram of velocity profile along the fracture due to the prevalence of inertial effect over viscous ones.

## Evidence of non-Darcy flow and non-Fickian transport in fractured media

C. Cherubini et al.

Title Page

Abstract

Introduction

Conclusions

References

Tables

Figures



Back

Close

Full Screen / Esc

Printer-friendly Version

Interactive Discussion



---

## Evidence of non-Darcy flow and non-Fickian transport in fractured media

C. Cherubini et al.

---

Title Page

Abstract

Introduction

Conclusions

References

Tables

Figures

⏪

⏩

◀

▶

Back

Close

Full Screen / Esc

Printer-friendly Version

Interactive Discussion



The linear-type relationship between velocity and dispersion for ADE and MIM models proves that for the range of flow rates imposed and for the selected path the geometrical dispersion dominates the mixing process along the fracture network.

The first order mass transfer  $\alpha$  and the mobile water fraction  $\beta$  coefficients show a different relationship with the velocity. The former assumes a constant value for low velocity, whereas it increases linearly in correspondence of  $v/\bar{L} = 1.5 \times 10^{-2} \text{ s}^{-1}$ . The latter shows a constant mean value of 0.56 for all range of velocity values.

For the range of flow rates observed the mass exchange between mobile and immobile zones is not negligible, the Damköhler varies in the range 0.4–1.

The MIM model proves to fit adequately the observed BTC. However, especially for low flow rate values the one-dimensional analytical MIM model does not fit properly the experimental BTCs, in fact a “late peak” is observed.

Further developments of this study would deal with investigating the performance of more accurate model (see Bodin et al., 2007) to predict tracer transport behavior in a fracture network. Moreover, in order to be able to generalize the relationships between models parameters different tracer tests will be carried out for each path of the model block.

Laboratory experiments give the advantage of improving the understanding of physical mechanisms under relatively well-controlled conditions, since the dependence of a physical process on different parameters can be tested and modeled.

Nevertheless, laboratory tests are characterized by relatively small temporal and spatial scales that pose the question on the representativity and transferability of laboratory data to the real system (“up-scaling”).

*Acknowledgements.* The authors would like to acknowledge the reviewers and the editor for their valuable comments and suggestions that helped improve the manuscript.

## References

- Aris, R.: On the dispersion of a solute in a fluid flowing through a tube, *P. R. Soc. Lond. A.*, 235, 67–77, 1956.
- Auriault, J. L. and Adler, P. M.: Taylor dispersion in porous media: analysis by multiple scale expansions, *Adv. Water Res.*, 18, 217–226, 1995.
- 5 Bahr, J. M. and Rubin, J.: Direct comparison of kinetic and local equilibrium formulations for solute transport affected by surface reactions, *Water Resour. Res.*, 23, 438–452, doi:10.1029/WR023i003p00438, 1987.
- Bear, J.: *Dynamics of Fluids in Porous Media*, Dover, New York, 1972.
- 10 Berkowitz, B., Kosakowski, G., Margolin, G., and Scher, H.: Application of continuous time random walk theory to tracer test measurements in fractured and heterogeneous porous media, *Ground Water*, 39, 593–604, 2001.
- Boschan, A., Ippolito, L., Chertcoff, R., Auradou, H., Talon, L., and Hulin, J. P.: Geometrical and Taylor dispersion in fracture with random obstacles: an experimental study with fluids of different rheologies, *Water Resour. Res.*, 44, W06420, doi:10.1029/2007WR006403, 2008.
- 15 Callahan, T. J., Reimus, P. W., Bowman, R. S., and Haga, M. J.: Using multiple experimental methods to determine fracture/matrix interactions and dispersion of nonreactive in saturated volcanic tuff, *Water Resour. Res.*, 36, 3547–3558, 2000.
- Chen, Z., Qian, J., and Qin, H.: Experimental study of the non-darcy flow and solute transport in a channeled single fracture, *J. Hydrodyn.*, 23, 745–751, 2011.
- 20 Cherubini, C. and Pastore, N.: Modeling contaminant propagation in fractured and karstic aquifer, *Fresen. Environ. Bull.*, 19, 1788–1794, 2010.
- Cherubini, C. and Pastore, N.: Critical stress scenarios for a coastal aquifer in southeastern Italy, *Nat. Hazards Earth Syst. Sci.*, 11, 1381–1393, doi:10.5194/nhess-11-1381-2011, 2011.
- 25 Cherubini, C., Giasi, C., and Pastore, N.: Fluid flow modeling of a coastal fractured karstic aquifer by means of a lumped parameter approach, *Environ. Earth Sci.*, Online ISSN: 1866-6299, 1–6, doi:10.1007/s12665-010-0851-5, 2010.
- Cherubini, C., Giasi, C. I., and Pastore, N.: Bench scale laboratory tests to analyze non-linear flow in fractured media, *Hydrol. Earth Syst. Sci.*, 16, 2511–2522, doi:10.5194/hess-16-2511-2012, 2012.
- 30 Crank, J.: *Mathematics of Diffusion*, Oxford University Press, New York, London, 1956.

---

### Evidence of non-Darcy flow and non-Fickian transport in fractured media

C. Cherubini et al.

---

Title Page

Abstract

Introduction

Conclusions

References

Tables

Figures

⏪

⏩

◀

▶

Back

Close

Full Screen / Esc

Printer-friendly Version

Interactive Discussion



---

## Evidence of non-Darcy flow and non-Fickian transport in fractured media

C. Cherubini et al.

---

Title Page

Abstract

Introduction

Conclusions

References

Tables

Figures

⏪

⏩

◀

▶

Back

Close

Full Screen / Esc

Printer-friendly Version

Interactive Discussion



Dullien, F.: Porous Media: Fluid Transport and Pore Structure, Academic Press, San Diego, 1992.

Goltz, M. N. and Roberts, P. V.: Three-dimensional solutions for solute transport in an infinite medium with mobile and immobile zones, *Water Resour. Res.*, 22, 1139–1148, 1986.

5 Leven, C., Sauter, M., Teutsch, G., and Dietrich, P.: Investigation of the effects of fractured porous media on hydraulics tests – an experimental study at laboratory scale using single well methods, *J. Hydrol.*, 297, 95–108, 2004.

10 Leven, C., Brauchler, R., Sauter, M., Teutsch, G., and Dietrich, P.: Flow and transport experiments conducted on laboratory block, in: *Flow and Transport in Fractured Porous Media*, edited by: Dietrich, P., Helmig, R., Hotzl, H., Kondeter, J., and Teutsch, G., Springer, Berlin, 174–197, 2005.

McDermott, C. I., Sauter, M., and Liedl, R.: New experimental techniques for pneumatic tomographical determination of the flow and transport parameters of highly fractured porous rock samples, *J. Hydrol.*, 278, 51–63, 2003.

15 Qian, J. Z., Chen, Z., Zhan, H. B., and Luo, S. H.: Solute transport in a filled single fracture under non-Darcian flow, *Int. J. Rock Mech. Min.*, 48, 132–140, 2011.

Rodrigues, N. E. and de Lima, J. L.: Solute transport in fractured media – analysis of non-reversibility in tracer tests, *Nonlinear Proc. Geoph.*, 15, 783–791, 2008.

20 Starr, R. C., Gillham, R. W., and Sudicky, E. A.: Experimental investigation of solute transport in stratified porous media: 2. The reactive case, *Water Resour. Res.*, 21, 1043–1050, doi:10.1029/WR021i007p01043, 1985.

Sudicky, E. A., Gillham, R. W., and Frind, E. O.: Experimental investigation of solute transport in stratified porous media: 1. The nonreactive case, *Water Resour. Res.*, 21, 1035–1041, doi:10.1029/WR021i007p01035, 1985.

25 Wagner, J. B. and Harvey, J. W.: Analysing the capabilities and limitation of tracer tests in stream – aquifer systems, in: *Impact of Human Activity on Groundwater Dynamics*, Proceedings of a symposium held during the Sixth IAHS Scientific Assembly at Maastricht, IAHS Publ. no. 269, 2001.

---

**Evidence of  
non-Darcy flow and  
non-Fickian transport  
in fractured media**

---

C. Cherubini et al.

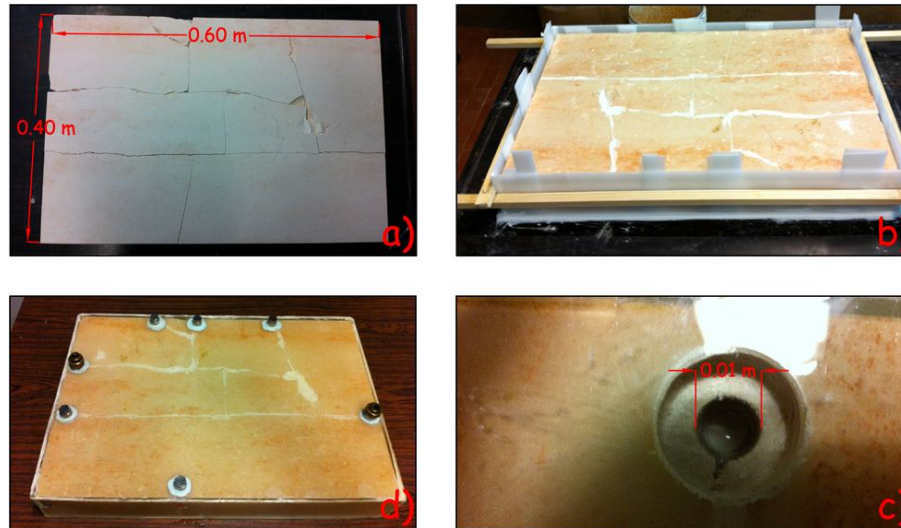


**Fig. 1.** (a) artificial discontinuities produced by means of 5 kg mallet blows; (b) epoxy resin casting; (c) example of a hole in correspondence of the edges of the discontinuities; (d) insertion of hexagonal bushing for the connection to the hydraulic circuit.

[Title Page](#)[Abstract](#)[Introduction](#)[Conclusions](#)[References](#)[Tables](#)[Figures](#)[⏪](#)[⏩](#)[◀](#)[▶](#)[Back](#)[Close](#)[Full Screen / Esc](#)[Printer-friendly Version](#)[Interactive Discussion](#)

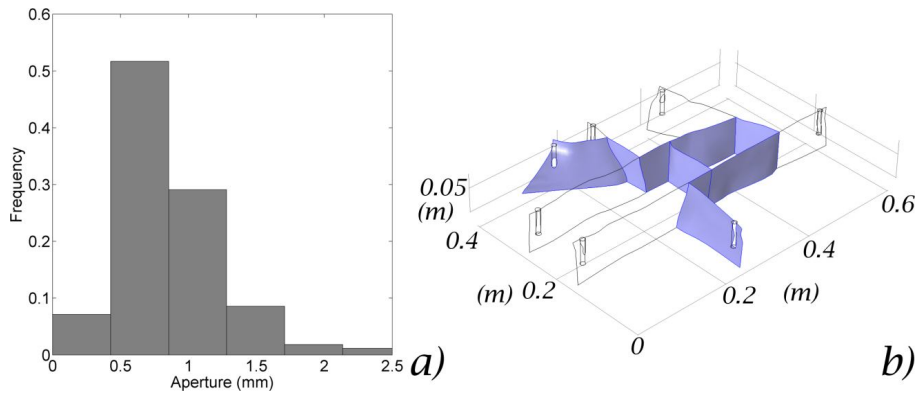


**Fig. 2. (a)** distribution of mechanical aperture evaluated on the 13688 samples **(b)** three dimensional reconstruction of the fracture network. The selected path is highlighted.

## Evidence of non-Darcy flow and non-Fickian transport in fractured media

C. Cherubini et al.

Title Page	
Abstract	Introduction
Conclusions	References
Tables	Figures
⏪	⏩
◀	▶
Back	Close
Full Screen / Esc	
Printer-friendly Version	
Interactive Discussion	

## Evidence of non-Darcy flow and non-Fickian transport in fractured media

C. Cherubini et al.

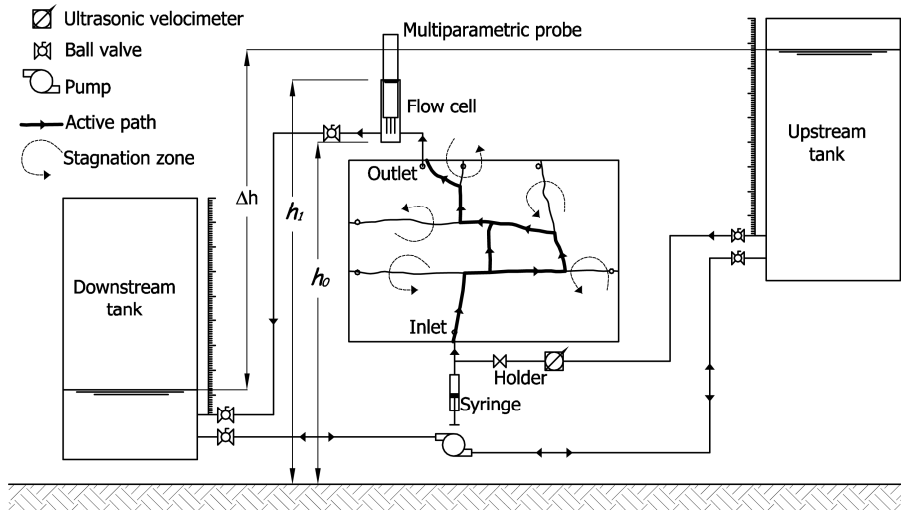


**Fig. 3.** Schematic diagram of the experimental setup.

Title Page

Abstract

Introduction

Conclusions

References

Tables

Figures

◀

▶

◀

▶

Back

Close

Full Screen / Esc

Printer-friendly Version

Interactive Discussion

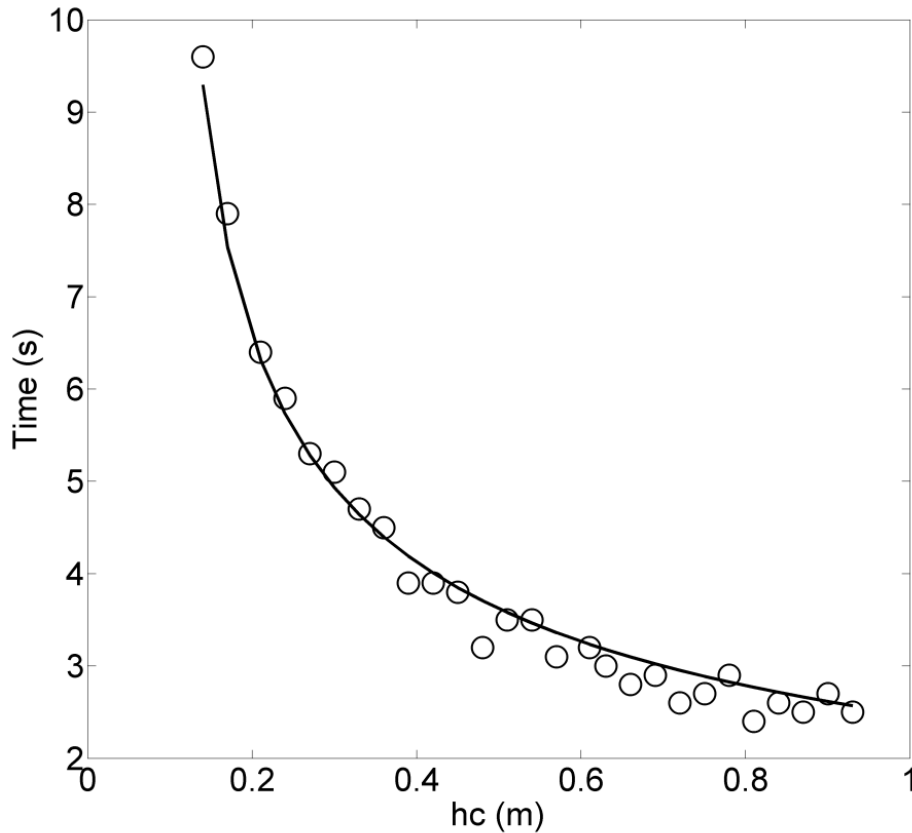


**Fig. 4.** Control head  $h_c$  vs. time for calibration of hydraulic circuit. Circle represents the experimental values obtained from tests carried out only on the hydraulic circuit. The marked line represents Eq. (22) with  $A$  and  $B$  equal to 0.

# HESSD

10, 221–254, 2013

## Evidence of non-Darcy flow and non-Fickian transport in fractured media

C. Cherubini et al.

Title Page

Abstract

Introduction

Conclusions

References

Tables

Figures



Back

Close

Full Screen / Esc

Printer-friendly Version

Interactive Discussion



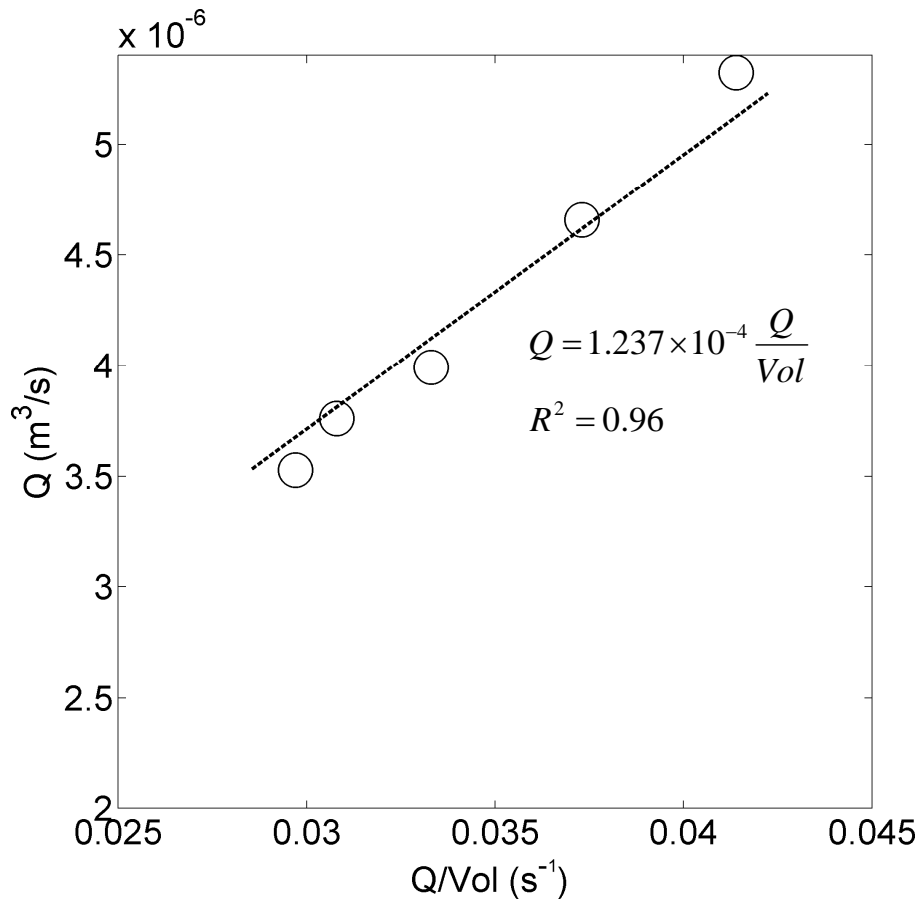


**Fig. 5.** Calibration of the probe.  $Q$  represents the measured flow rate,  $Q/Vol$  is estimated by fitting the BTCs curves of the probes. The circle line represents the experimental values, the dashed line represents the linear regression.

## Evidence of non-Darcy flow and non-Fickian transport in fractured media

C. Cherubini et al.

Title Page

Abstract	Introduction
Conclusions	References
Tables	Figures

◀	▶
◀	▶
Back	Close

Full Screen / Esc

Printer-friendly Version

Interactive Discussion



## Evidence of non-Darcy flow and non-Fickian transport in fractured media

C. Cherubini et al.

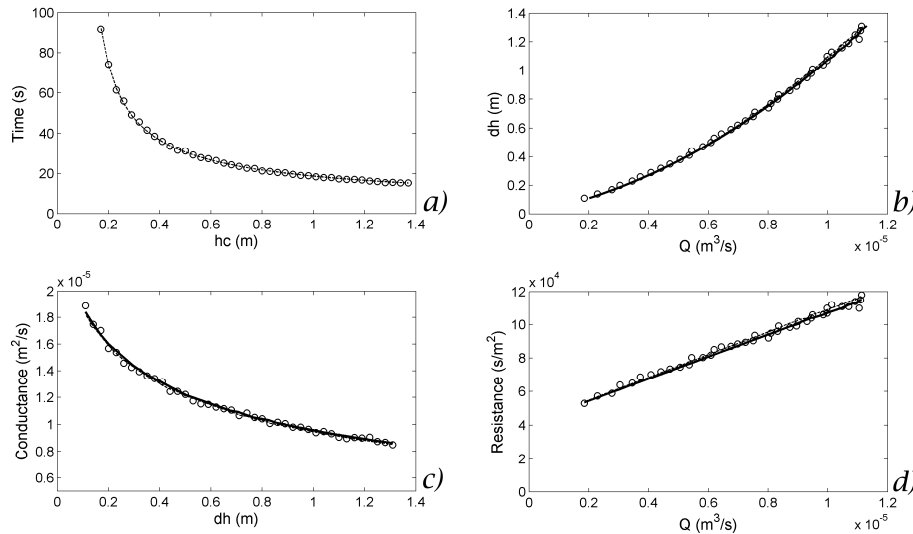


**Fig. 6.** Experimental results obtained for the hydraulic test performed on the selected path **(a)** Control head  $h_c$  vs. time. **(b)** average flow rate  $Q$  (Eq. 19) vs. difference head (Eq. 20) **(c)** difference head vs. conductance term (Eq. 21) **(d)** average flow rate  $Q$  vs. resistance term evaluated as the inverse of conductance. The circle represents the experimental values, the dashed line represents the fitting of experimental values, the marked line represents the functions without the effect of circuit.

[Title Page](#)
[Abstract](#)
[Introduction](#)
[Conclusions](#)
[References](#)
[Tables](#)
[Figures](#)
[⏪](#)
[⏩](#)
[◀](#)
[▶](#)
[Back](#)
[Close](#)
[Full Screen / Esc](#)
[Printer-friendly Version](#)
[Interactive Discussion](#)

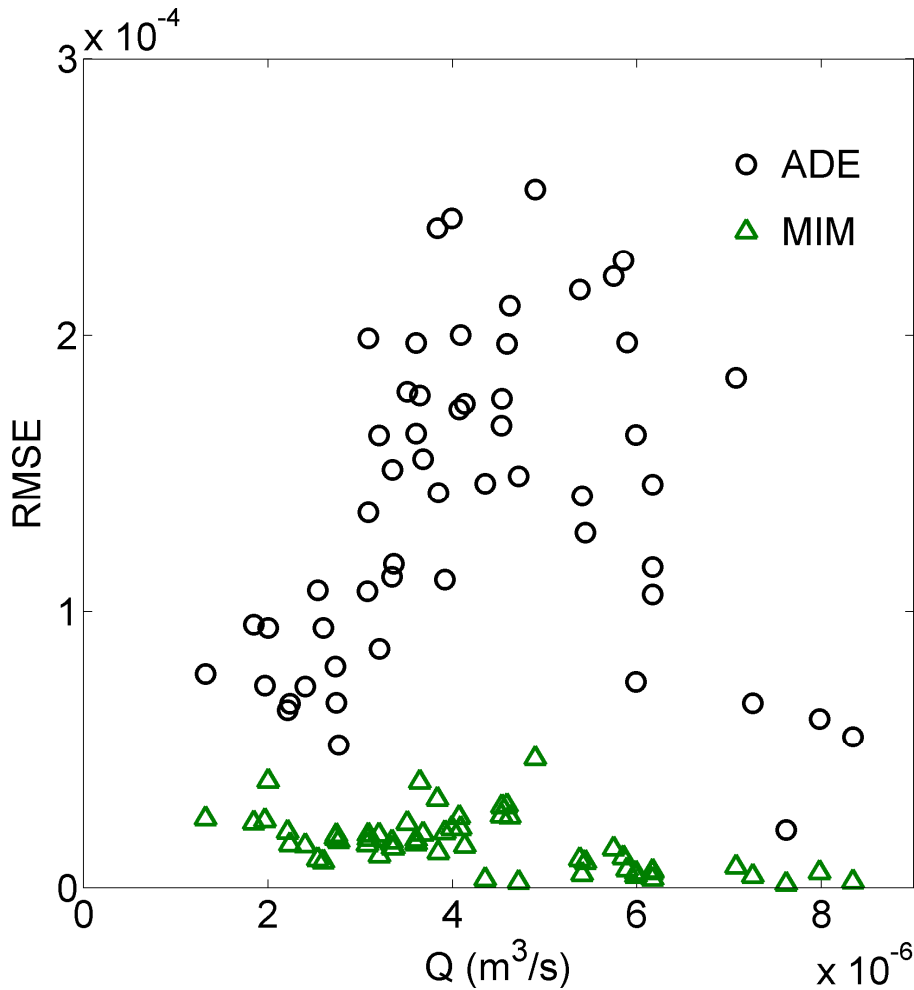


Fig. 7. Flow rate vs. RMSE for ADE and MIM model.

## Evidence of non-Darcy flow and non-Fickian transport in fractured media

C. Cherubini et al.

Title Page

Abstract	Introduction
Conclusions	References
Tables	Figures

⏪
⏩

◀
▶

Back	Close
------	-------

Full Screen / Esc

Printer-friendly Version

Interactive Discussion



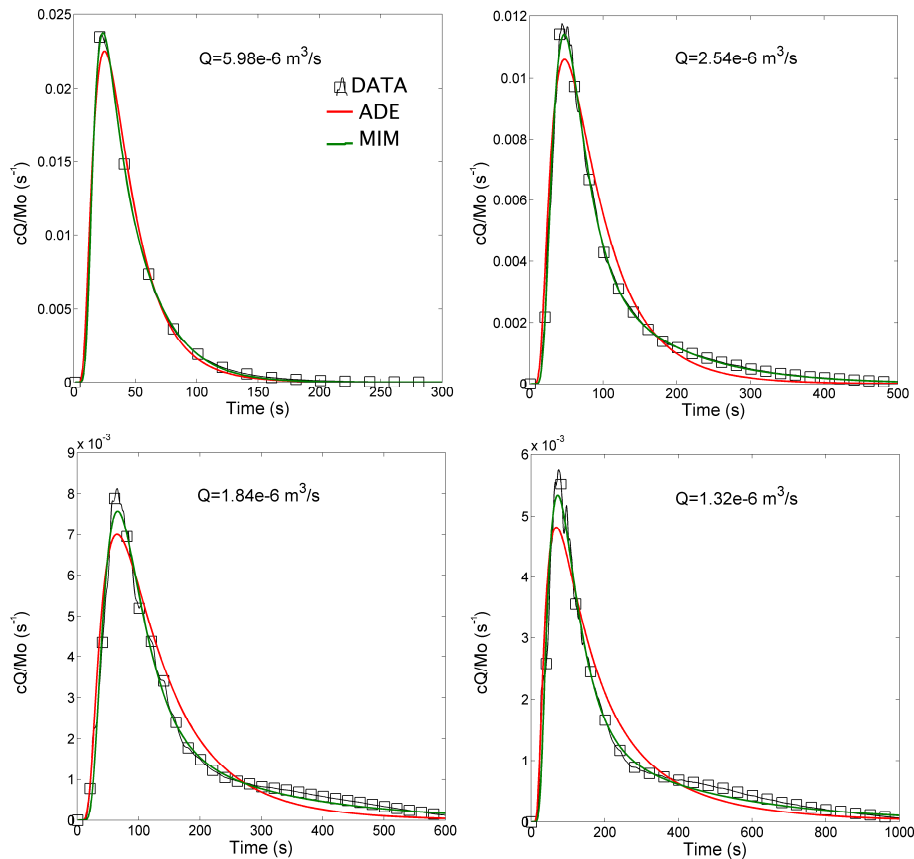


**Fig. 8.** Fitting of BTCs for different flow rate values. The squares represent the experimental values, the red and green line are the analytical solution for ADE and MIM model, respectively.

## Evidence of non-Darcy flow and non-Fickian transport in fractured media

C. Cherubini et al.

Title Page

Abstract

Introduction

Conclusions

References

Tables

Figures

◀

▶

◀

▶

Back

Close

Full Screen / Esc

Printer-friendly Version

Interactive Discussion



## Evidence of non-Darcy flow and non-Fickian transport in fractured media

C. Cherubini et al.

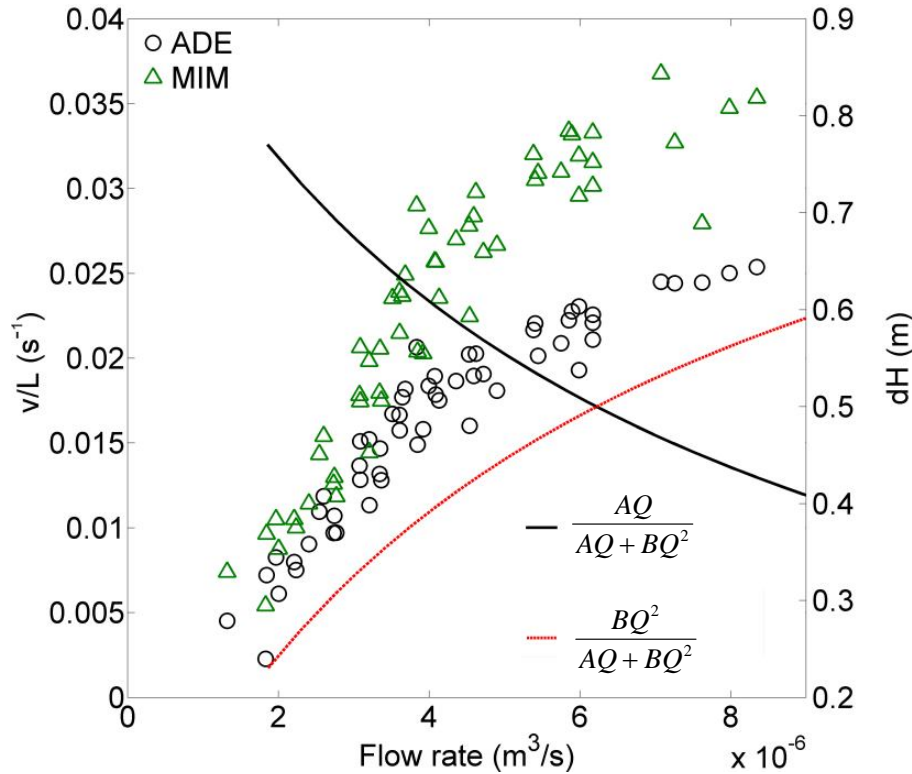


**Fig. 9.** Flow rate vs. the ratio of linear and non linear losses to total loss and flow rate vs. normalized average flow velocity estimated for ADE and MIM model.

Title Page

Abstract	Introduction
Conclusions	References
Tables	Figures

⏪
⏩

◀
▶

Back
Close

Full Screen / Esc

Printer-friendly Version

Interactive Discussion

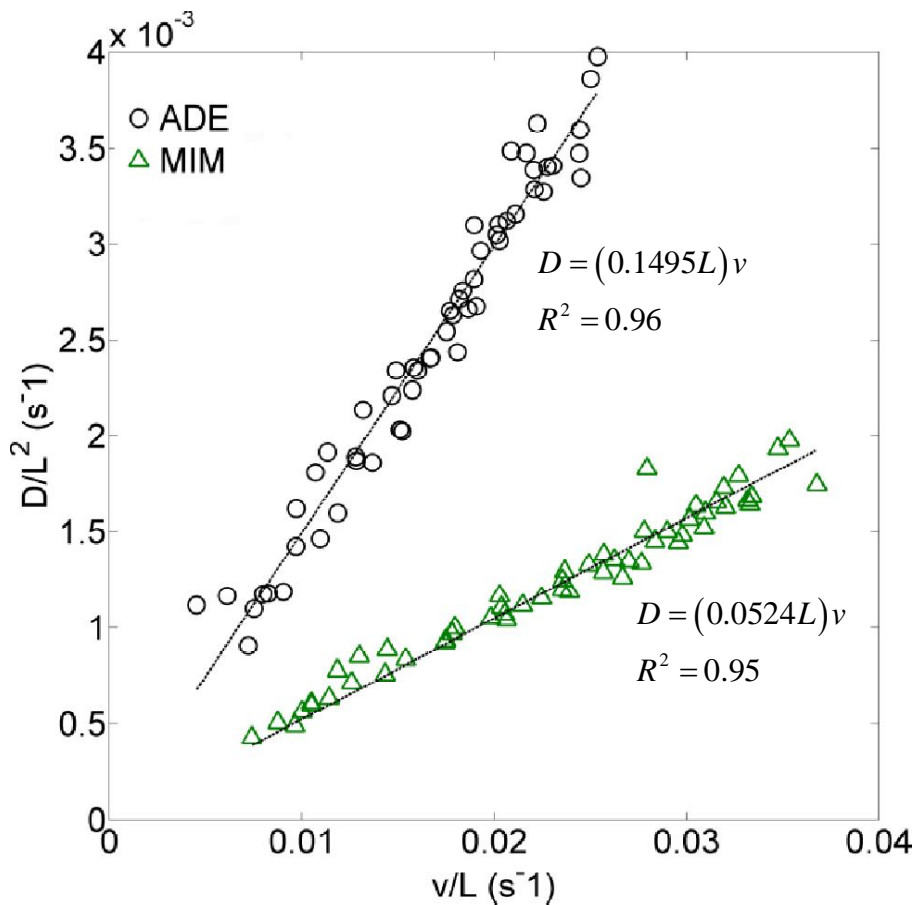


**Fig. 10.** Normalized flow velocity vs. normalized dispersion estimated for ADE and MIM model.

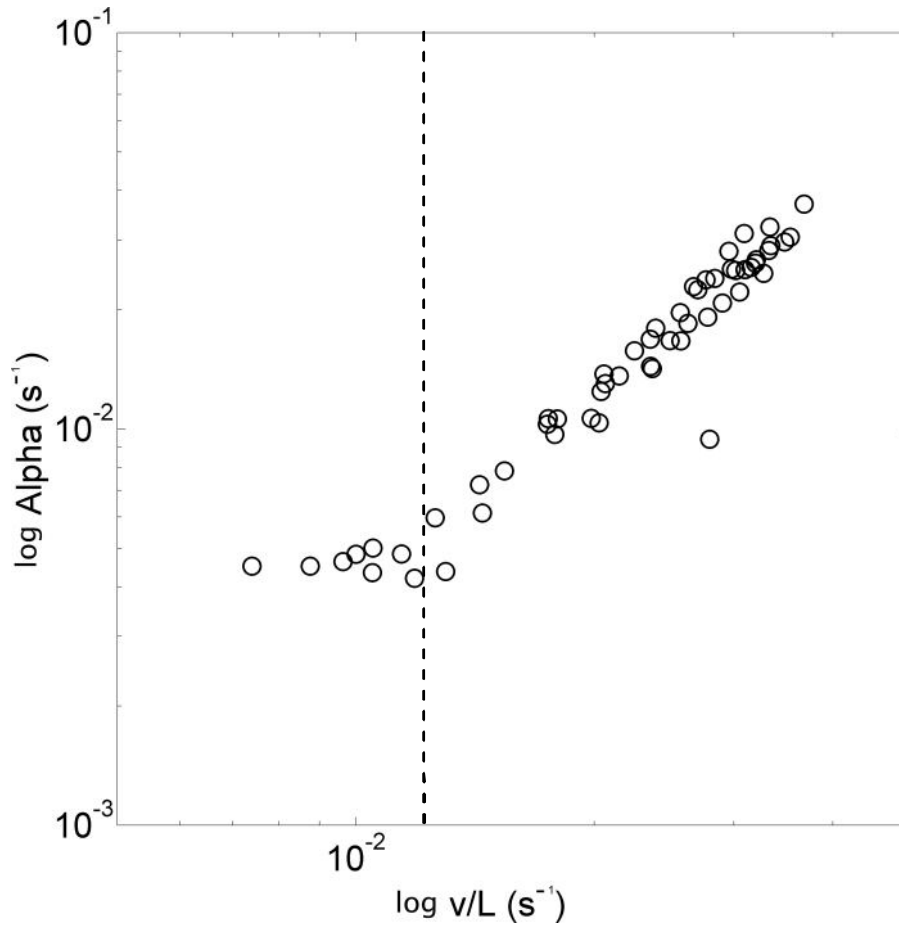


**Fig. 11.** Normalized flow velocity vs. first order mass exchange coefficient  $\alpha$  estimated for MIM model.

## Evidence of non-Darcy flow and non-Fickian transport in fractured media

C. Cherubini et al.

Title Page

Abstract

Introduction

Conclusions

References

Tables

Figures

◀

▶

◀

▶

Back

Close

Full Screen / Esc

Printer-friendly Version

Interactive Discussion

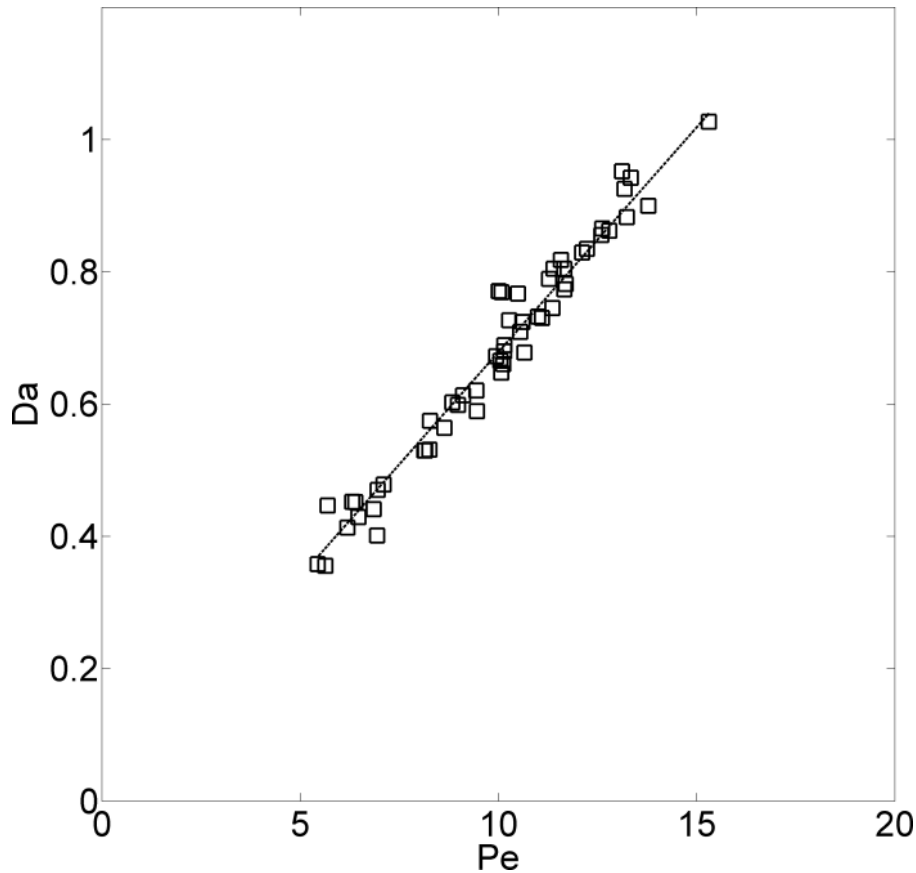


**Fig. 12.** Péclet number vs. Damköhler number.

# HESSD

10, 221–254, 2013

## Evidence of non-Darcy flow and non-Fickian transport in fractured media

C. Cherubini et al.

- Title Page
- Abstract
Introduction
- Conclusions
References
- Tables
Figures
- ⏪
⏩
- ◀
▶
- Back
Close
- Full Screen / Esc
- Printer-friendly Version
- Interactive Discussion

